An Experimental Safety Study for Stab/Puncture and Incised Wounds

By Sami Haddadin, Alin Albu-Schäffer, Fahed Haddadin, Jürgen Roßmann, and Gerd Hirzinger

1070-9932/11/$26.00©2011 IEEE

Soft-Tissue Injuries in Robotics

This article details the analysis of soft-tissue injuries caused by sharp tools that are mounted on/grasped by a robot [1]. The evaluation is considered as the next step down the road to a complete safety analysis of robots for human–robot interaction (HRI). We conduct an analysis of soft-tissue injuries based on available biomechanical and forensic data and present various experimental results with biological tissue for validation. Furthermore, possible countermeasures are proposed and evaluated by means of measurable injury reduction.

Motivation and State of the Art

Currently, increasing effort is taken in the robotics community to understand injury mechanisms during a physical HRI. This is motivated by the fact that human and robot will work intensively and closely together, and therefore, one has to be aware of the potential threats in case such a close cooperation takes place. There are two fundamental classes of contact-related injuries:

1) blunt impact injury
2) sharp contact injury.

Until now, only blunt impacts were investigated in the robotics literature [see Figure 1(a)], leaving open the question of what can happen if a robot with an attached sharp tool on impacts with a human [cf. Figure 1(b)]. If robots are allowed to work and help humans, they must be able to handle potentially dangerous tools and equipment. Tasks may range from slicing bread (see Figure 2) or preparing some meal to fulfilling the duties of a craftsman. This desired coexistence of humans and robots poses a serious safety problem that needs to be solved. Naturally, the reservation against robots handling sharp tools in human environments is enormously high. Industrial standards and obligations are generally very restrictive [2]. Until a robot will actually fulfill complex helper tasks in domestic environments using sharp tools, massive safety investigation is necessary. An important class of injuries to be analyzed in this context are soft-tissue injuries, of which the typical ones are described in the "Soft-Tissue Injury Caused by Sharp Tools" section. They range from usually less dangerous injuries as contusions or abrasions to very painful lacerations and even life-threatening ones such as stab/puncture wounds. Stab/puncture wounds are usually more lethal than laceration. However, for very sensitive zones, e.g.,

Digital Object Identifier 10.1109/MRA.2011.942996
Date of publication: 8 December 2011

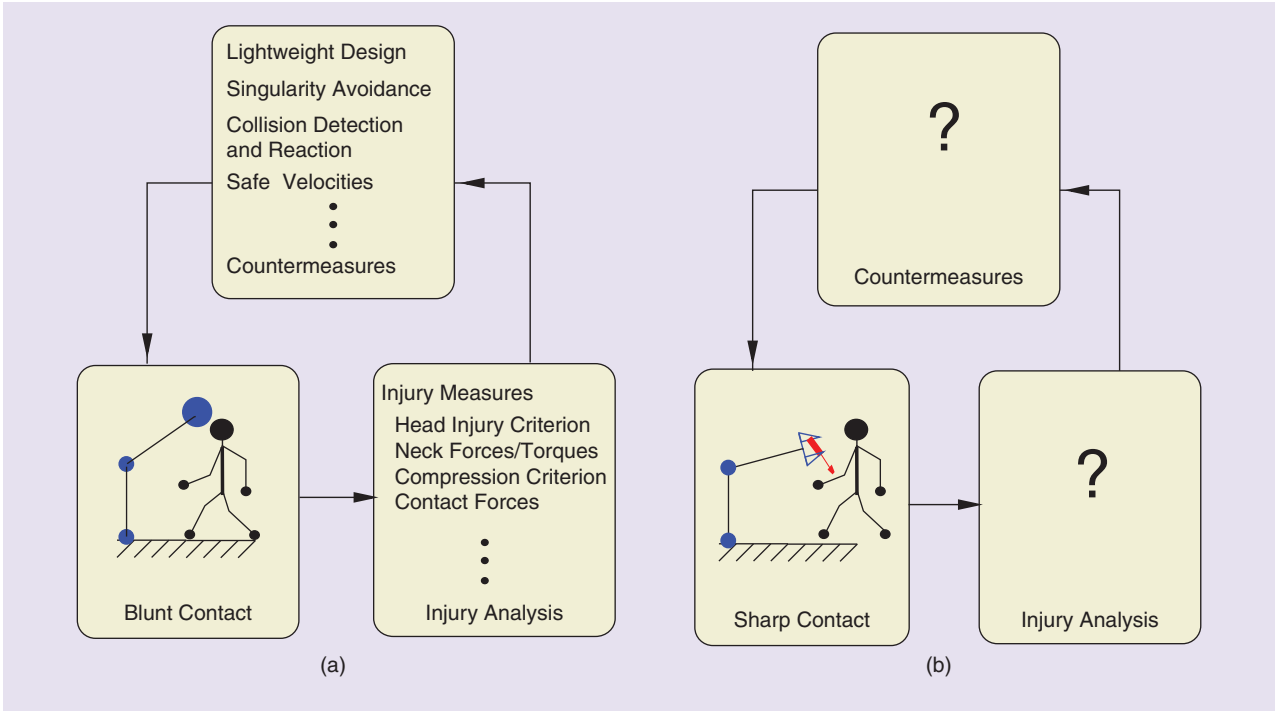

Figure 1. (a) Current status of injury analysis in robotics. Mainly, the effect of blunt impacts was investigated. (b) The analysis of soft-tissue injury caused by sharp objects is still a largely open field. Neither injury analysis nor appropriate countermeasures have been investigated yet.

around the area of the underlying arteria carotis, deep cuts can be equally dangerous.

Although several countermeasures, criteria, and control schemes for safe physical HRI were proposed in the literature [3]–[9], the main objective of actually quantifying and evaluating them on a biomechanical basis was marginally addressed. First evaluations in this direction were carried out in [10], where the human pain tolerance was estimated on the basis of human experiments. In this work, the somatic pain was considered as a suitable criterion for determining a safety limit against mechanical stimuli. In [11] and [12], further attempts to overcome this drawback were mainly carried out in simulation, and recently in [13]–[15], an exhaustive evaluation of blunt impacts with various human body parts was carried out. Earlier work presented in [16] focused on a more abstract injury classification. The authors presented a first classification and hazard analysis, however, at this time, lacking in biomechanical motivation and experimental validation. In particular, they assumed an exhaustive protection of the human for the given concept. Reference [17] also discussed robot safety in human environments and pointed out the various potential threats.

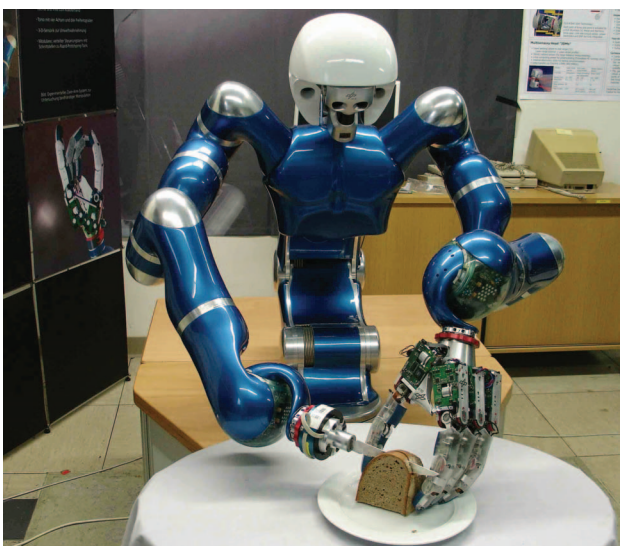

Figure 2. Future service robots are supposed to work with possibly dangerous tools. How can we make robots safe for such tasks?

So far, the fundamental question of what is the resulting injury of a human during undesired contact was not discussed and analyzed in depth in the context of soft-tissue injury. Especially, the human biomechanics, injury tolerance, and injury severity were not considered or discussed on a quantitative basis. Previous works [6], [16] already introduced and analyzed skin stress as an injury index for assessing soft-tissue injury. Nevertheless, a real focus shift to the mentioned soft-tissue injuries was not carried out [18], [19]. In [18], the need for a complete evaluation of soft-tissue injury was given. In this work, the maximum curvature of a robot colliding with a human is approximated with a sphere. This is used to analyze the maximum tensile stress, which in turn is the basis to distinguish between safe and unsafe contact. In [19], a classification and synopsis of possible injuries in HRI was given. The influence of the different parameters and properties of the robot and the environment on the resulting injury severity was discussed,

and various injury indices, e.g., contact force or energy density, were proposed.

Generally, soft tissue injury analysis in robotics was mainly model based so far. Knowing from our experience how uncertain and contestable simple models (and their parameterization) for such complex biomechanical processes are, we decided to treat this topic empirically and acquire real data for injury thresholds. We think that these experiments provide reliable facts and can constitute a help for further evaluation and validation of models.

Several aspects are treated in this article, leading to three main contributions:

1) to evaluate soft-tissue injuries caused by various possibly dangerous tools, we deal with stab/puncture and incised wounds
2) to prove the effectiveness of our collision detection and reaction schemes for the Lightweight Robot III (LWR-III) of the German Aerospace Center (DLR) with soft-tissue and volunteer tests; these countermeasures give us the possibility to drastically reduce the injury potential during stabbing and prevent even the slightest cutaneous injury during cutting
3) to provide empirically relevant limit values for injury prevention for the case of sharp contact.

Soft-Tissue Injury Caused by Sharp Tools

Biomechanics of Soft-tissue Injury

Sharp contact can cause various characteristic injuries in the context of robotics. The most important ones are abrasions, contusions, lacerations, incised wounds, and puncture wounds.

- Abrasions or excoriations are the ablation of parts or the entire epidermis from the corium.
- Contusions are basically bleedings into tissue that can be found in the skin, muscles, and inner organs.
- A laceration can be described as a tear in the tissue, i.e., the tissues are torn apart and remain irregular.
- An incised wound is a transection in skin continuity which is wider than it is deep. This is especially the result of a cut.
- A puncture or stab/puncture wound on the other hand is usually characterized by being deeper than it is wide.

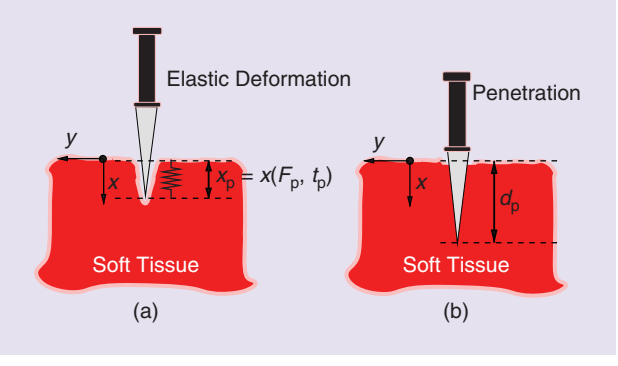

Figure 3. (a) Elastic deformation of the skin before penetration up to x_p at a force level of F_p. (b) Penetration depth d_p into the tissue after exceeding the tolerance force F_p.

In this article, we focus on stab/puncture wounds and incised wounds/cuts in order to capture the vast threat posed by sharp tools such as knifes, scalpels, or scissors and leave the low-severity injuries for future research. (We are currently preparing systematic drop-testing experiments to analyze the biomechanics of such injury.)

The influence of underlying bones is neglected, and the evaluation focuses on areas such as the abdomen or thigh. This can be considered as a worst-case scenario since the underlying soft tissue is very sensitive and a bone would reduce the possible injury severity by means of penetration depth (apart from the case of slipping or impinging). If, e.g., an object hits the human thorax above the heart location and penetrates further, it is possible to hit a heart-protecting rib. In case the object neither slips nor impinges nor exerts forces that are able to cause rib fracture, the possible injury is limited from the tissue to the rib and further rib injury (e.g., penetration into the rib). This is of course significantly less dangerous if the robot tip penetrated between the two ribs and reached the cardiac tissue. The analysis of these relaxed situations is left for future work.

Stab/puncture wounds were investigated in the forensic literature with different knives, and it was concluded that strain is not an appropriate measure to define the tolerance value for knives and similar tools because the contact area is too small [20]–[22]. Instead, the evaluation of the penetration force F_p is proposed, which in our opinion, is well suited to be used in the context of robotics as well. Tolerance forces depend on the layers of clothing and range according to [21] between

- $F_p^1 = 76 \pm 45$ N for uncovered skin
- $F_p^2 = 173$ N for three layers of a typical clothing.

Furthermore, the tolerance force correlates to a skin deflection x_p at which the actual penetration takes place. This deflection is

- $x_p^1 = 1.24 \pm 0.49$ cm for naked skin
- $x_p^2 = 2.26 \pm 0.61$ cm for multilayered clothes. (This evaluation was carried out at low velocities by determining the static stab force. However, in [22], dynamic tests were conducted and produced similar numerical values. In [23], stab tests with three different knives led to significantly lower penetration values.)

In this article, we assume the relationship to be linear in first approximation. Therefore, the skin can be modeled by a stiffness before penetration and a tolerance force that corresponds to the moment of penetration (Figure 3). Therefore, we assume the following contact model

$$K_{H,i} = \begin{cases} \frac{F_p^i}{x_p^i} & F_{\text{ext}} < F_p^i, \\ 0 & F_{\text{ext}} \geq F_p^i, \end{cases} \tag{1}$$

where F_{ext} is the contact force acting on the human and robot, respectively. What happens after the knife actually penetrates is to our knowledge still not investigated yet and needs further treatment and evaluation. The first hints

given in [22] show that a second resistance after the initial skin penetration can be observed. As a first indicator, we considered the intrusion/penetration depth d_p to be a relevant quantity (of course depending on the location where the skin is actually penetrated and its underlying tissue) in our experiments to evaluate the severity of injury.

According to [24], no similar investigation of incised wounds/cuts was carried out. This is presumably due to the nonexisting forensic necessity. In this sense, our analysis will bring new insights to the understanding of this injury mechanism in a broader sense and is not limited to robotics.

Next, we present the results on depth measurements of vital organs, since we believe this is a relevant injury indicator that is applicable to robotics in the sense that it provides inherent minimum requirements on the robot-braking distance.

The Depth of Vital Organs

To quantify potentially lethal stabs, we conducted ultrasonic measurements with ten human subjects to estimate the distance from the skin surface to the surface of the human heart. Between the fourth and fifth intercostellar spaces, the depth is measurable since the heart abuts on the thorax wall. Numerical values of $d_{\text{heart}} = 2.2$–2.7 cm were measured with a mean of $\bar{d}_{\text{heart}} = 2.4$ cm.

In addition to the initial heart depth analysis, we conducted measurements for several vital organs. (The measurements had no diagnostic nor therapeutical purposes and did not cause any injury. The subjects were anonymous. The ultrasonic system used a ESAOTE Megas, yoc 2005. We use a 7.5-MHz probe for the throat and neck soft tissues and a 3.5-MHz probe for the other organs.) The mean results of the depth measurements are as follows:

- Or1: heart, 2.2 cm
- Or2: abdominal aorta, 6.0 cm
- Or3: liver (side), 2.0 cm
- Or4: liver (subcostal), 3.7 cm
- Or5: kidney (back), 5.0 cm
- Or6: soft tissue throat (right), 1.3 cm
- Or7: soft tissue throat (left), 1.3 cm
- Or8: subclavia, 1.6 cm
- Or9: milt, 3.8 cm.

The short distances clearly point out how vulnerable human organs are as soon as penetration occurs.

Since it is very difficult to estimate the particular injury a human would suffer from sharp contact, we believe it is important to define the requirements for robot design and control, which quantify the benefit one would, e.g., obtain from a collision detection and reaction strategy in an intuitive manner. An important value that is a natural candidate is the maximum braking distance of a robot.

Braking Distance

As shown in the previous subsection, the organ depth d_{organ} is an intuitive number that can be used as a minimum braking distance, which absolutely needs to be ensured during sharp robot–human contact.

External contact forces caused by the human dynamic response potentially decrease the braking distance, especially, for low inertia robots. Therefore, the worst-case braking distance is present without taking this into consideration. It consists of three phases:

1) nominal motion before collision detection triggers (system delay, detection sensitivity): $t_0 \rightarrow t_1$
2) nominal motion before stopping reaction strategy activates (system latencies): $t_1 \rightarrow t_2$
3) stopping motion till entire stop of the system (actuator dynamics/saturation): $t_2 \rightarrow t_3$.

Therefore, the overall braking distance that needs to be smaller than d_{organ} is

$$||x_{\text{stop}}|| = \int_{t_0}^{t_2} \dot{x}_{\text{nom}}\, dt + \int_{t_2}^{t_3} \dot{x}_{\text{brake}} dt < d_{\text{organ}}. \quad (2)$$

This limit is from our perspective a good choice to qualify the effectivity of collision detection and reaction schemes, since it is an absolute limit before a life-threatening injury occurs if penetration into the body takes place. It inherently defines the minimum performance characteristics on joint torque dynamics by means of maximum joint torque and response time.

After the introduction of necessary biomechanical/forensic definitions and our performance/injury measure, the used collision detection and reaction methods are briefly overviewed. Furthermore, their use as a countermeasure to soft-tissue injury caused by sharp tools is motivated by a simulation since it initially seemed not very realistic to be able to prevent, e.g., injuries caused by knives and scalpels. While the detection and reaction strategies are the outcome of a joint work in cooperation with the University of Rome [4], [25], the present article uses this as a tool for a biomechanical evaluation of possible soft-tissue injuries with and without collision detection.

Collision Detection and Reaction

Countermeasures against soft-tissue injury can be manifold, but a crucial feature has to be the effective physical collision detection and reaction. An important aspect is to decide whether a detected interaction force for the robot is currently fulfilling a desired task (e.g., preparing food) or constitutes a potential threat. However, from our point of view, this is a question of higher-level planning and human motion detection involving external sensing, e.g., a vision system. This separate topic is clearly out of the scope of this article. A rather simple scheme for distinguishing whether the occurring collision is part of the assembly task or a collision with the human could be to switch the collision detection off as soon as clamping of the human can be excluded. This can be ensured if the distance between the tool and the known environment (table) is lower than a threshold. In this situation, a very good world model is of course necessary, which could be the case in an industrial scenario.

Generally, as soon as a collision is identified, various reaction schemes could be activated. In case of mounted sharp tools, this reaction scheme needs to be treated very carefully, since activating, e.g., the strategy of a free-floating compliant robot, is still a dangerous threat with a mounted (or grasped) knife (of course, a reduced one compared with a robot moving in position control).

The DLR Lightweight Robot III

In our evaluation, we conducted simulations and experiments with the LWR-III. The LWR-III is a 7 degrees-of-freedom lightweight robot with 1.1 m reach, moderately flexible joints (due to the use of harmonic drives and joint torque sensors), and was explicitly developed for the direct physical interaction and cooperation with humans. Its total weight is 15 kg and the nominal payload is 7 kg. (Please note that the robot is able to carry its own weight of 7 kg for research applications.) Furthermore, it is equipped with joint torque sensors in each joint, enabling the sensing of external contact forces along the entire robotic structure. For details concerning the full design of the robot, please refer to [26] and [27].

Compared with the soft-tissue properties of the used subjects during the investigated collisions throughout this article, the robot is very stiff. Thus, thresholds of penetration forces and other properties obtained by our measurements are not valid only for this particular robot but can directly be applied to other robots.

Collision Detection

The collision detection used in this work was introduced and analyzed in [4], [28], and [25]. Its basic concept is to observe the generalized momentum $\mathbf{p} = \mathbf{M}(\mathbf{q})\dot{\mathbf{q}}$, as proposed in [7] and [29], with $\mathbf{M} \in \mathbb{R}^{n \times n}$ being the manipulator mass matrix and $\mathbf{q}, \dot{\mathbf{q}} \in \mathbb{R}^n$ the link position and velocity. It can be proven that the observed disturbance $\widehat{\mathbf{r}}$ is a componentwise filtered version of the real external torque $\boldsymbol{\tau}_{\text{ext}} \in \mathbb{R}^n$, i.e., $\widehat{\mathbf{r}} \approx \boldsymbol{\tau}_{\text{ext}}$. This enables us to detect contact along the entire structure of the robot without additional external sensing. The collision threshold $\boldsymbol{\delta}_c \in \mathbb{R}^n$ (ideally, $\boldsymbol{\delta}_c = \mathbf{0}$) is mainly due to sensor noise and model uncertainties. For the real LWR-III, this corresponds to $\boldsymbol{\delta}_c = 0.03\boldsymbol{\tau}_{\max}$, i.e., 3% of the maximum nominal torque, $\boldsymbol{\tau}_{\max} \in \mathbb{R}^n$, of the robot. (For the LWR-III, the maximum nominal joint torques are $\boldsymbol{\tau}_{\max} = [180\ 180\ 80\ 80\ 80\ 35\ 35]^T$ N·m). This value indicates that very low contact forces can be detected.

Collision Reaction

After a collision is detected and isolated, we instantaneously trigger an appropriate collision reaction scheme.

$$\boldsymbol{\tau}_d = \begin{cases} \boldsymbol{\tau}_{d,\text{nom}} & \forall i : |\hat{r}_i| < \boldsymbol{\delta}_{c,i}, \\ \boldsymbol{\tau}_{d,\text{col}} & \exists |\hat{r}_i| \geq \boldsymbol{\delta}_{c,i}, \end{cases} \tag{3}$$

where $\boldsymbol{\tau}_{d,\text{nom.}}$ is the nominal torque input for motion control and $\boldsymbol{\tau}_{d,\text{col}}$ depicts the control input for an appropriate reaction scheme. Various strategies were proposed in [4] and [28], and three of them are tested and compared in this article for soft-tissue contact (silicone, pig) with sharp tools. One goal is to be able to evaluate the effectivity of the detection in a critical scenario. As discussed in the "Safety Experiments" section, the collision detection can make the difference between serious, even, lethal injuries and no injury at all. The investigated collision strategies are

- *Strategy 0*: Keep the reference movement, i.e., show no reaction at all and continue to follow $\theta_{\boldsymbol{d}}$, where $\theta_{\boldsymbol{d}} \in \mathbb{R}^n$ is the desired motor position. This is the reference behavior.
- *Strategy 1*: Stop the robot as soon as a collision is detected, meaning to set $\theta_{\boldsymbol{d}} = \theta(t_{\boldsymbol{c}})$, where $\theta \in \mathbb{R}^n$ is the motor position and t_c is the instance of collision detection.
- *Strategy 2*: Switch from position control to zero-gravity torque control [30], [31] and let the robot react in a convenient and compliant manner.

Before presenting the experiments, a simulation use case is discussed, which was our initial motivation for evaluating collision detection and reaction for a robot that moves such dangerous tools.

A Simulation Use Case with the LWR-III

Here, the penetration of the human skin with a knife and its prevention is treated. A simple and reasonable contact model for stabbing is available as mentioned in the "Soft-Tissue Injury Caused by Sharp Tools" section. We use the model for the fully covered human, i.e., $F_p^2 = 173$ N and $x_p^2 = 2.26 \pm 0.61$cm. For simulating the stabbing process, the following elastic joint model is assumed. (For the LWR-III, the nonnegligible joint elasticity between motor and link inertia due to the harmonic drive gears and the joint torque sensor has to be taken into account into the model equation, leading to the standard flexible joint model proposed in [32]):

$$M(\mathbf{q})\ddot{\mathbf{q}} + C(\mathbf{q}, \dot{\mathbf{q}})\dot{\mathbf{q}} + \mathbf{g}(\mathbf{q}) = \boldsymbol{\tau}_J + \boldsymbol{\tau}_{\text{ext}}, \tag{4}$$

$$B\ddot{\boldsymbol{\theta}} + \boldsymbol{\tau}_J + \boldsymbol{\tau}_F = \boldsymbol{\tau}_m, \tag{5}$$

$$\boldsymbol{\tau}_J = K_J(\boldsymbol{\theta} - \mathbf{q}), \tag{6}$$

with $\boldsymbol{\theta} \in \mathbb{R}^n$ being the motor side position, $\boldsymbol{\tau}_{\boldsymbol{J}} \in \mathbb{R}^n$, $\boldsymbol{\tau}_{\boldsymbol{F}}$ the elastic joint and friction torque, $K_J = \text{diag}\{K_{J,i}\} \in \mathbb{R}^{n \times n}$ the diagonal positive definite joint stiffness matrix, and $B = \text{diag}\{B_i\} \in \mathbb{R}^{n \times n}$ the diagonal positive definite motor inertia matrix. The controller is the full-state feedback controller from [30]. $\boldsymbol{\tau}_{\text{ext}}$ is associated with the (generalized) Cartesian collision force $\mathcal{F}_{\text{ext}}$ by

$$\boldsymbol{\tau}_{\text{ext}} = J_c^T(\mathbf{q})\mathcal{F}_{\text{ext}}, \tag{7}$$

where $J_c(\mathbf{q})$ is the (geometric) contact Jacobian. The force $\mathcal{F}_{\text{ext}}$ is generated by (1). (Please note that we assume no change in behavior due to penetration in the simulation. In

other words, a constant stiffness model is used.) The human soft tissue is modeled as a virtual wall with the already mentioned spring constant and is assumed to be clamped, i.e., a worst-case scenario is treated. The robot is mounted on a fixed base. The maximum joint velocity of the robot is 120°/s, and the desired motion is a straight line with reconfiguration from elbow up to elbow down. The maximum Cartesian velocity results from the maximum joint velocity in the fourth joint, whereas the second and the seventh joint drive at half the velocity, resulting in a maximum Cartesian velocity of 0.64 m/s. In this simulation, the Cartesian impact velocity was chosen to be $\dot{\mathbf{x}}_R \in \{0.16\ 0.32\ 0.64\}$ m/s for the fully covered skin. In Figure 4, the results of the contact forces are shown. Clearly, the effectiveness of the collision detection and reaction is apparent even for high Cartesian velocities. Severe injury can be caused after penetration of the skin without any collision reaction. On the other hand, the skin is not penetrated for active strategies since the robot is able to react sensitive and fast enough to prevent the human from being hurt. Furthermore, the properties of the collision reaction strategies become apparent: Strategy 1 actively stops the robot and reduces the contact force significantly faster than does Strategy 2. On the other hand, the switch in control (Strategy 2) reduces the contact force down to zero in contrast to Strategy 1. This is due to the passive behavior of the robot in a torque-controlled mode with gravitation compensation. Even for 0.64 m/s, the collision detection is able to prevent damage of the skin. Figure 4 (a) shows the results for a joint velocity of 30°/s, 4 (b) 60°/s, and 4 (c) 120°/s in the fourth (elbow) joint. 120°/s is the current maximum joint velocity of the LWR-III.

This simulation shows how easy it is to penetrate the human skin even with a robot moving at moderate speeds and the human being protected by three layers of clothing. Penetrating the human skin itself seems to be a marginal injury, but at the same time, there are various vital organs such as the heart or the liver located relatively close to the body surface (see "The Depth of Vital Organs" section).

Based on these observations, a combination of both strategies seems to be the best choice. This could be realized using Strategy 1 for stopping the penetration quickly (and minimizing the force profile) and then switch to torque control with gravity compensation (Strategy 2) for being compliant after having stopped. This would prevent clamping of the human after the collision as one can easily push the robot away. An implementation example of a more complex behavior is shown in Figure 5. The depicted example is a possible implementation for the free space motion with a three-stage reaction strategy. Initially, the robot state is in its wait state W. After receiving the Go command a desired free motion task is performed in state R. If a slight collision (HF = 1) is detected in R the robot reacts to it by switching to Strategy 1 that is performed by state S_1. In S_1 the kinetic energy E_{kin} of the robot is monitored and when this drops below the predefined threshold ϵ the robot switches to state S_2, i.e., to reflex Strategy 2. Now the robot behaves compliant and can be easily pushed away or moved to a desired location by the human. If the human operator confirms (CF = 1) the robot leaves the reaction strategy and switches back to the wait state W. Apart from this nominal collision behavior, the robot is also able to react with an emergency strategy if a very severe collision was observed (FT1 = 1). When switching to S_3 the robot engages its brakes and waits for human initiative. The operator may now actively confirm the robot to switch to its nominal wait state W again.

After this discussion on collision detection and reaction, various experiments that are presented next provide insight about the injury mechanisms during contact with various sharp tools.

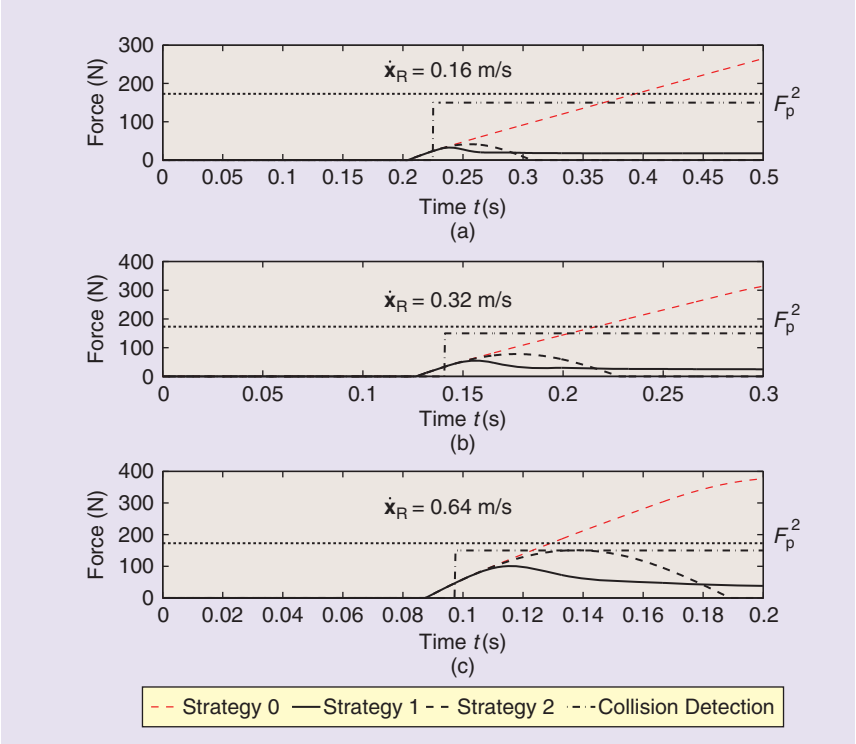

Figure 4. Stabbing simulation with the full dynamic model of the LWR-III equipped with a knife. The fully covered human stands 0.3 m before the stretched out singularity of the robot. F_p^2 denotes the penetration force for the fully covered skin.

Safety Experiments

In this section, various experiments are presented and the injury severity

possibly occurring if a robot with a sharp tool penetrates a soft material is analyzed. The dynamics of such an impact is especially worth being investigated since, during rigid (unconstrained) collisions [13], the dynamics is so fast that a realistic robot is not able to reduce the impact characteristics by the collision detection and reaction. However, during our previous investigations, a subjective safe feeling could be definitely experienced by the users. Despite this limitation in reactivity to blunt impacts, it was shown that the necessity of countermeasures is not absolutely crucial since rigid free impacts pose only a very limited risk at the typical robot velocities up to 2 m/s. This is definitely not the case for soft-tissue injuries caused by a stab because the injury severity due to penetration can reach lethal dimensions. The particular worst case depends on the exact location by means of potentially injured underlying organs. Because of the much slower dynamics compared with rigid impacts, the requirements on a reactive robot concerning detection and reaction speed are somewhat relaxed and not unachievable for such situations as exemplified in the "A Simulation Use Case with the LWR-III" section. It seems surprising at first glance that it is not possible to counterbalance rigid blunt robot–human impacts by means of controls that are definitely not life threatening, but at the same time, dangerous or even lethal contacts with tools seem manageable to a certain extent. (Please note that we refer to impact speeds of up to 2 m/s.) One purpose of the present experiment is to prove this statement.

In the framework of this article, the situation in which the robot moves in position control with/without collision detection by utilizing joint torque sensing is considered. The contact force is measured with a JR3 force–torque sensor in the wrist. Please note that this sensor is only used for measurement and not for collision detection.

Investigated Tools

The variety of tools one could analyze are basically countless and, therefore, a representative selection of tools with different sharpness was carried out (Figure 6). Up to now, there is no benchmarking test of tools, since the underlying biomechanics is not fully understood yet. Therefore, we chose typical household objects such as knives of different sharpness, a scalpel, and a screwdriver. These tools were selected as a reasonable choice of potentially dangerous ones one could think of in robotic applications. They were removed from their original fixtures and glued into new mountings. Therefore, a fixed connection between the tool and a robot can be guaranteed, and no compliance reduces the transferred forces. This selection enables us to test a wide range of cuts and stabs with varying blade characteristics and sharpness. Currently, we are preparing a systematic biomechanical test to provide a set of benchmarking objects for investigating soft-tissue injury. The tools were tested in the same condition they were bought, except for the fact that they were glued into a rigid mounting to remove eventually beneficial compliances.

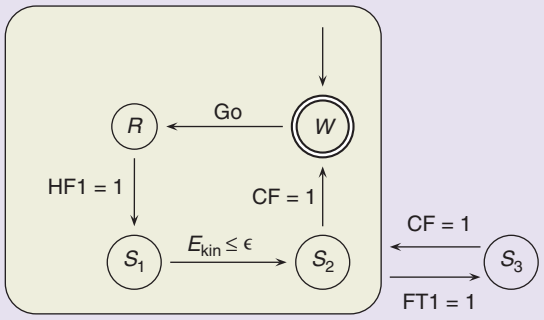

	Symbol	Meaning
States	W	Wait State
	R	Running State
	S_1	Collision Strategy 1 State
	S_2	Collision Strategy 2 State
	S_3	Collision Strategy 3 State
Events	Go	Go Event for Starting Process
Signals	HF1	Collision of Severity-Level HF1
	FT1	Collision of Severity-Level FT1
	E_{kin}	Kinetic Energy of the Manipulator
	ϵ	Kinetic Energy Threshold

Figure 5. Combining the different collision reaction techniques to complex reflex behaviors.

Silicone Block

As a first experimental contact material, a silicone block was used to get a feeling for the sensitivity and effectiveness of the collision detection and reaction for soft contact. (The used silicone was Silastic T2 with a Shore hardness of A40.) These first tests were conducted at a Cartesian velocity of 0.25 m/s, which is the recommended velocity according to International Standards Organization (ISO) 10218 for collaborative robots [2]. The mounted tool is the kitchen knife. The desired goal configuration was located at a depth of 8 cm in the silicone block. Without any reaction strategy, the achieved penetration was 35 mm at a contact force of 220 N with

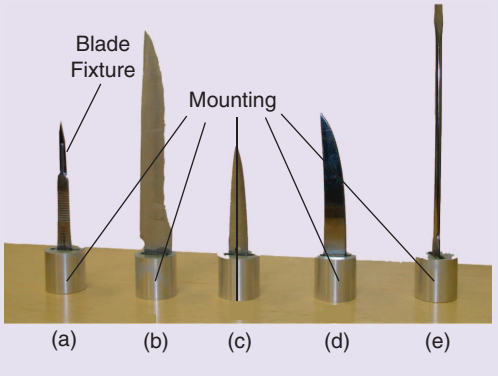

Figure 6. Investigated tools: (a) Scalpel, (b) kitchen knife, (c) scissors, (d) steak knife, and (e) screwdriver.

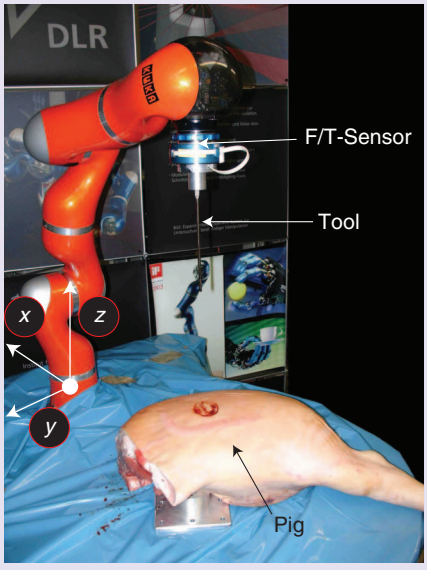

Figure 7. Testing setup for the pig experimental series. The robot is equipped with a JR3 force/torque sensor for measuring the contact force. The tools are rigidly mounted to the robot such that no significant additional compliance is introduced.

joint six exceeding its maximum joint torque. This causes a low-level safety feature for robot protection to immediately stop the manipulator by engaging its brakes. With activated collision detection and reaction, the maximum penetration depth was significantly reduced to $\leq$6 mm at a contact force of 40 N, i.e., a reduction by a factor of $\approx$ 5.

Pig Experiments

To obtain results with real biological tissue, we conducted experiments with a pig leg (Figure 7). From an anatomical point of view, pigs are commonly accepted as being similar to human beings. The stabbing trajectory is a straight line along the z axis and the desired configuration is slightly above the table. The pig is located on a rigid table, i.e., a clamping scenario is analyzed because of its worst-case properties. Both impact experiments in automobile crash testing and forensic medicine use these for first experiments or even for predictions of results with human tissue. Differences to humans and changing tissue properties through mortex and room temperature are apparent but yet it seems to be of immanent importance to conduct experiments with natural tissue. To our understanding, these investigations can be fundamental to robotic safety since classical impact experiments with knives in forensic medicine [21], [22] did (of course) not take any robot behavior into account, which, in turn, vastly influences the resulting injury.

Stabbing

Table 1 and Figure 8 summarize the outcome of the stabbing tests. The trajectory of the robot was chosen such that it moves on a straight vertical line along the z axis (cf. Figure 7) contacting the skin in normal direction with the tool axis. The investigated robot velocities were 0.16 and 0.64 m/s. Each experiment with Strategy 1 or 2 was carried out two to three times. The results were very similar during independent trials with an error of maximum 5% in the force profile. Surprisingly, with the screwdriver mounted, the robot was not able to penetrate the pig skin at all. For this tool, the maximum nominal joint torques

Table 1. The results of the stabbing experiments.

		$\dot{\mathbf{x}}_R = 0.16$ m/s					$\dot{\mathbf{x}}_R = 0.64$ m/s				
Exp. No.	Tool	Strategy	d_p(mm)	t_p (ms)	F_p (N)	x_p (mm)	Exp. No.	d_p(mm)	t_p (ms)	F_p (N)	x_p(mm)
A1.1	Steak knife	0	full	100	15	14	A1.2	Full	14	11	10
A2.1		1	None/4	—	—	—	A2.2	22	14	11	10
A3.1		2	3–5	100	15	14	A3.2	64	14	11	10
B1.1	Scissors	0	Full	195	60	25	B1.2	Full	47	65	29
B2.1		1	None	—	—	—	B2.2	18	34	45	21
B3.1		2	None	—	—	—	B3.2	42	42	65	25
C1.1	Kitchen knife	0	98	240	76	29	C1.2	135	55	73	32
C2.1		1	None	—	—	—	C2.2	1	48	60	29
C3.1		2	None	—	—	—	C3.2	18	55	76	31
D1.1	Scalpel	0	Full	50	5	8	D1.2	Full	15	5	10
D2.1		1	17	50	5	8	D2.2	17	15	5	10
D3.1		2	17	50	5	8	D3.2	39	15	5	10

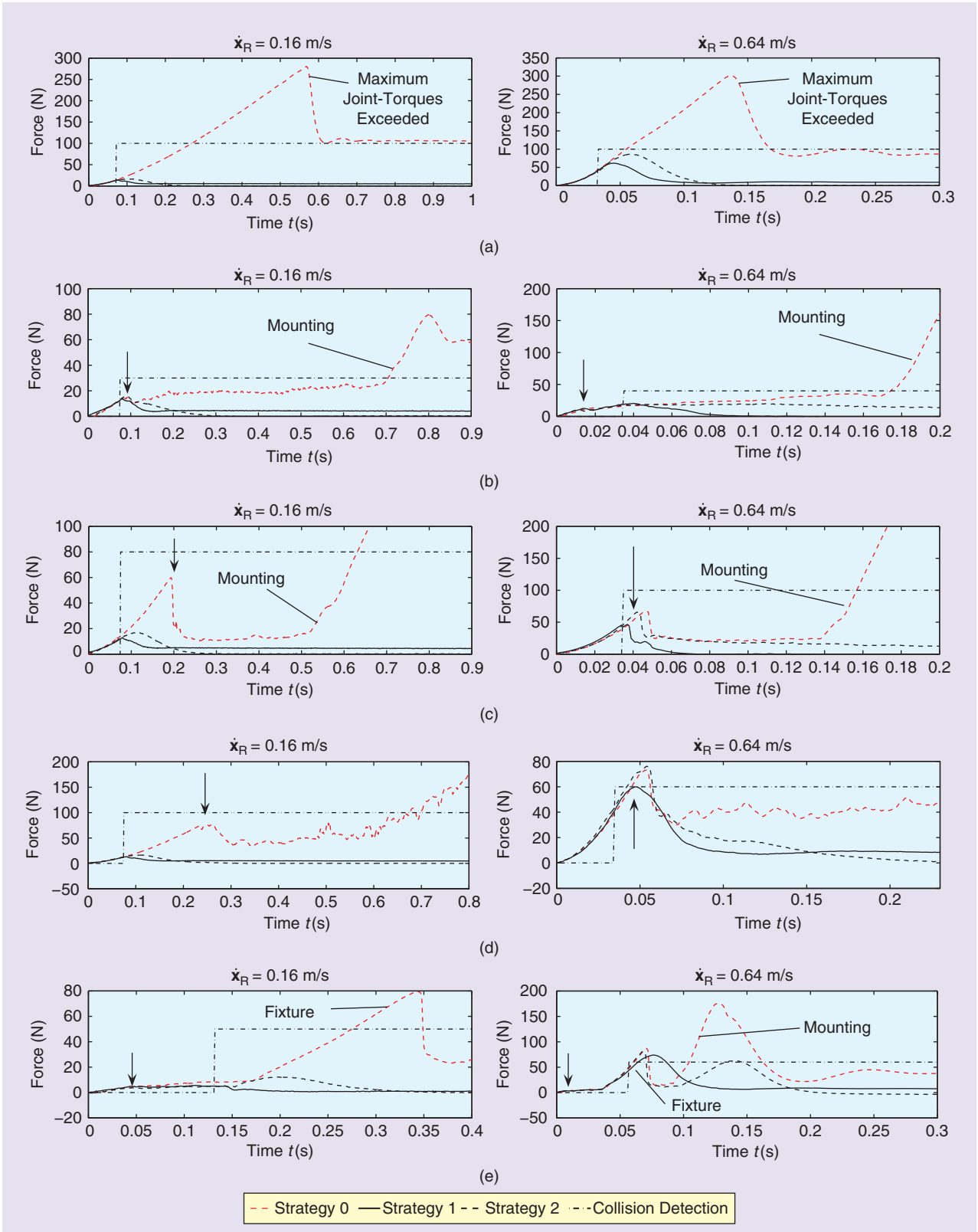

Figure 8. Results of stabbing tests with and without collision detection for the pig tests. (a) screwdriver, (b) steak knife, (c) scissors, (d) kitchen knife, and (e) scalpel. The arrows denote the moment of penetration.

always exceeded, and a low-level safety mechanism engaged the brakes of the robot, as described in the "Silicone Block" section. For the other tools, Table 1 gives the measured values for the penetration depth d_p, the penetration time t_p (which can be interpreted as the available reaction time to prevent skin penetration), the penetration force F_p, and finally, the elastic deflection before penetration x_p, i.e., the deflection of the skin that has to be reached with a particular tool for penetration (Figure 3).

The observed penetration forces for the scissors and the kitchen knife correlate strongly to the ones reported in the "Soft-Tissue Injury Caused by Sharp Tools" section. On the other hand, for the sharp steak knife and the scalpel, significantly lower values are observed. This strongly recommends to extend the given analysis to more general classes of objects.

As shown in Table 1 for the case without collision detection (Strategy 0), all sharp tools penetrate into the tissue with their entire blade length, pointing out the lethality potential. At the same time, it can be expected that, at low speeds, a very good chance of detection and reaction exists, and, especially for the kitchen knife and the scissors, a full injury prevention seems possible. For the steak knife, the success depends on the exact location and ranges from no penetration up to a penetration depth of a few millimeters. For the used scalpel, there is actually no real chance to detect the penetration of the blade. The collision detection is only triggered by the fixture of the blade that has a significantly larger cross section (Figure 6).

For larger velocities, a significant observation, confirming the results from the simulation, can be made: Switching to Strategy 2 is causing a higher penetration depth due to its passive behavior. Because the robot behaves in this control mode as a free-floating mass with a certain amount of initial kinetic energy further penetration of the tissue until the robot's energy is fully dissipated takes place. Moreover, only Strategy 1 is able to limit the penetration depth below the values that are lethal in absolute worst-case scenarios, i.e., below 2.4 cm. Quite surprisingly, the penetration force does not seem to be velocity dependent for a particular knife.

Apart from the characteristic values in Table 1, the force profiles of the stabbing experiments are depicted in Figure 8: (a) shows the obtained graphs for the screwdriver, (b) the steak knife, (c) the scissors, (d) the kitchen knife, and (e) the scalpel. The force–time evolution is plotted for all three strategies. Especially, the following aspects become clear when evaluating the plots.

- The moment of penetration is characterized by a significant force discontinuity (drop).
- A very low resistance can be observed from the moment the tool intruded the subcutaneous tissue.
- Force reduction by Strategy 2 is significantly slower compared with Strategy 1 (compare with "A Simulation Use Case with the LWR-III" section).
- After the initial penetration, the contact force increases slowly compared with the elastic force of the skin.
- All experiments with the kitchen knife (this is a comparable knife as the one used in [20]–[22]) show penetration close to 76 N, as stated in the "Soft-Tissue Injury Caused by Sharp Tools" section.

The influence of tool mounting (see Figure 6) can be observed for Strategy 0, resulting in a dramatic increase in force and a compression of the entire subject (the tool mounting establishes a blunt contact). In case of the scalpel, the quite different course needs to be explained a bit: The low penetration threshold is followed by an almost constant section, which represents the intrusion of the entire blade. For 0.16 m/s, the following increase in force is caused by the fixture of the blade which can be detected. For the graph with an impact velocity of 0.64 m/s, the force increase due to the fixture is followed by a second one caused by the mounting as for the previous tools.

Table 2 lists the results with respect to each organ and whether the respective limit penetration would have been reached or not. Again, we see that the stopping strategy is the most effective strategy that is able to prevent severe penetration.

Cutting

The second injury mechanism that is investigated in this article is cutting. The pure cut trajectory with a fixed object can be described by the tool orientation ϕ_1, the desired cut direction ϕ_2, and the cutting velocity (Figure 9). If ϕ_1 is chosen, then the pig position is already determined since the cut shall be carried out with the full available blade length. In our case, ϕ_1 was chosen to be $\phi_1 = 30^\circ$. Investigated tools were the steak knife, the scalpel, and the kitchen knife. The question for which the cutting angle ϕ_2 is the worst case was answered experimentally and led to $\phi_2 = 10^\circ$. Please note that the subject is fixed, presumably leading to higher injuries compared with a nonfixed subject. Furthermore, it became clear to us that the cutting velocities must be quite high to cause damage to the skin and the underlying tissue. At a low velocity of $||\dot{\mathbf{x}}_{\text{cut}}|| = 0.25$ m/s, more or less no injury was observed, and merely a scratch in the skin could be found. However, at $||\dot{\mathbf{x}}_{\text{cut}}|| = 0.8$ m/s this changed dramatically: Figure 10(a) shows the large and deep incisions caused by all tools if no safety feature is activated. Life-threatening depths can be easily accomplished. Apparently, the blade length is heavily influencing the resulting laceration depth. Although a scalpel is an extraordinary sharp tool easily penetrating the skin, the small blade length limits the penetration depth to 14 mm. This is almost an order of magnitude smaller than for the large kitchen knife. Thus, for such high velocities, long-blade knifes are far more dangerous than e.g., scalpels, which in turn are able to penetrate the skin at quite low velocities. On the left column, the caused laceration depths at 0:8 m/s are indicated. All tools easily penetrated the tissue and cutting depths of up to 101 mm are reached. Such depths are lethal and would pose an enormous threat. On the right column, the effect

Table 2. The resulting injury for stabbing experiments (see the "The Depth of Vital Organs" section labeling).

Exp. No. (Str.)	Or1	Or2	Or3	Or4	Or5	Or6	Or7	Or8	Or9
A1.1(0)	×	×	×	×	×	×	×	×	×
A1.2(0)	×	×	×	×	×	×	×	×	×
A2.1(1)	✓	✓	✓	✓	✓	✓	✓	✓	✓
A2.2(1)	✓	✓	✓	✓	✓	×	×	×	✓
A3.1(2)	✓	✓	✓	✓	✓	✓	✓	✓	✓
A3.2(2)	×	×	×	×	×	×	×	×	×
B1.1(0)	×	×	×	×	×	×	×	×	×
B1.2(0)	×	×	×	×	×	×	×	×	×
B2.1(1)	✓	✓	✓	✓	✓	✓	✓	✓	✓
B2.2(1)	✓	✓	✓	✓	✓	×	×	×	✓
B3.1(2)	✓	✓	✓	✓	✓	✓	✓	✓	✓
B3.2(2)	×	✓	×	×	✓	×	×	×	×
C1.1(0)	×	×	×	×	×	×	×	×	×
C1.2(0)	×	×	×	×	×	×	×	×	×
C2.1(1)	✓	✓	✓	✓	✓	✓	✓	✓	✓
C2.2(1)	✓	✓	✓	✓	✓	✓	✓	✓	✓
C3.1(2)	✓	✓	✓	✓	✓	✓	✓	✓	✓
C3.2(2)	✓	✓	✓	✓	✓	×	×	×	✓
D1.1(0)	×	×	×	×	×	×	×	×	×
D1.2(0)	×	×	×	×	×	×	×	×	×
D2.1(1)	✓	✓	✓	✓	✓	×	×	×	✓
D2.2(1)	✓	✓	✓	✓	✓	×	×	×	✓
D3.1(2)	✓	✓	✓	✓	✓	×	×	×	✓
D3.2(2)	×	✓	×	×	✓	×	×	×	×

of reacting to a collision is apparent. The robot stops as soon as a collision was detected (Strategy 1). No cut could be observed. These tests show that we can reduce the injury level from lethal to none.

Though large and potentially fatal injuries are possible, the risk can be reduced even at 0.8 m/s by collision detection and reaction to almost negligible levels at which no penetration or cut takes place anymore. Even in case of the scalpel, we are able to entirely prevent injury of the epidermis, pointing out the surprisingly high sensitivity of our collision detection [cf. Figure 10(b), (d), and (f)].

Figure 11 depicts the force, position, and velocity profiles for the cut motion. The forces are mainly acting in the $({}^{w}x, {}^{w}z)$-plane (Figure 9). The figure shows measurements for Strategies 0 and 1. Again, we observe the effectiveness of detection. At $t \approx 1.08$ s, we observe the beginning of a zagged behavior, which corresponds to the penetration event. The corresponding contact force is ≈ 80 N. With Strategy 1 activated, such large forces are prevented.

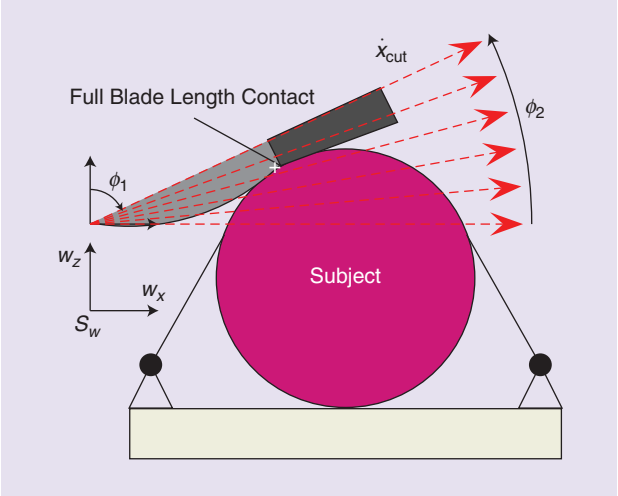

Figure 9. Cutting trajectories for a fixed subject. ϕ_1 is the tool orientation and ϕ_2 the cutting direction. The tool is positioned such that the blade origin contacts the subject. Thus, the full blade length can be used for cutting the tissue. S_w denotes the world coordinate frame.

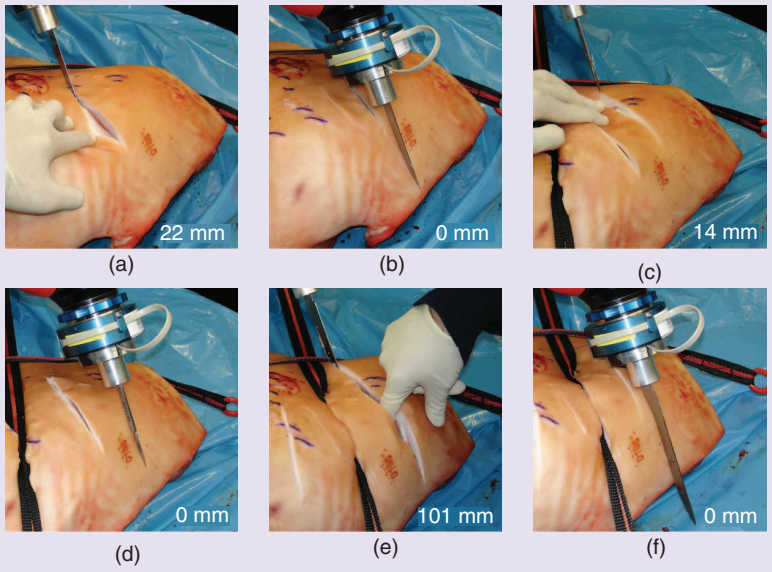

Figure 10. Resulting injury due to cutting with a (a) and (b) steak knife, (c) and (d) scalpel, and (e) and (f) kitchen knife.

The following conclusions for cutting can be drawn:

1) Injuries caused by cutting can reach severe if not lethal levels at high velocities. At low velocities, the epidermis is hardly injured.
2) The achieved level of injury mainly depends on the blade length and the cutting velocity.
3) Collision detection based on joint torque sensing is an effective countermeasure to entirely prevent injuries from cutting at quite high velocities.

After this in-depth evaluation of soft-tissue injuries caused by sharp tools, we were confident to exemplify the effectiveness of collision detection with a human volunteer.

The Most Convincing Argument

Since the presented experiments showed promising results and proved how reliably one is able to promptly detect and react to collisions, some measurements are shown, where a human holds his arm in free space against the moving robot with a mounted knife (Figure 12). (The human volunteer was happy to participate in this test series and did this of free will.) A full evaluation for the case of free stabbing has to be carried out, but it is definitely less dangerous compared with the constrained stabbing presented in this article. The robot velocity was chosen to be $\dot{\mathbf{x}}_R \in \{0.15\ 0.25\ 0.5\ 1.0\}$ m/s. In Figure 13, the measured force during the collision with the human is plotted. Because of collision detection, the

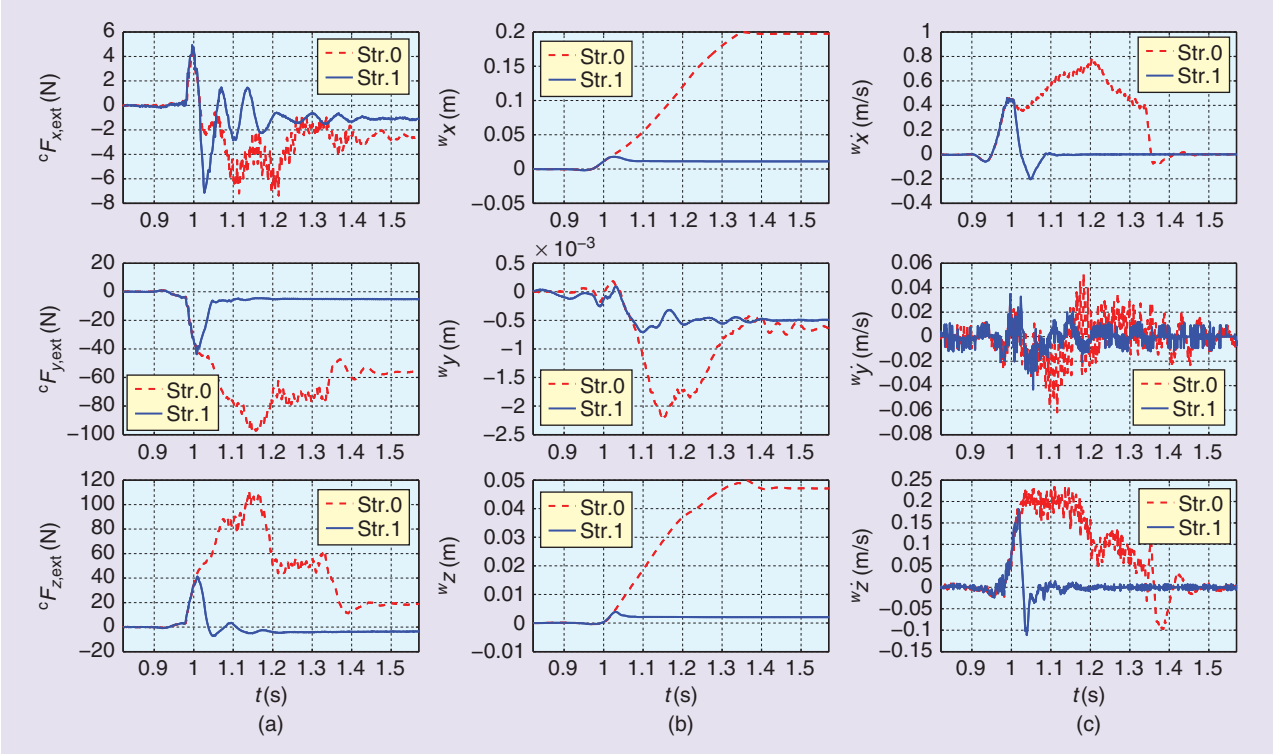

Figure 11. Time evolution of cutting with and without collision detection. (a) Contact force, (b) position, and (c) velocity.

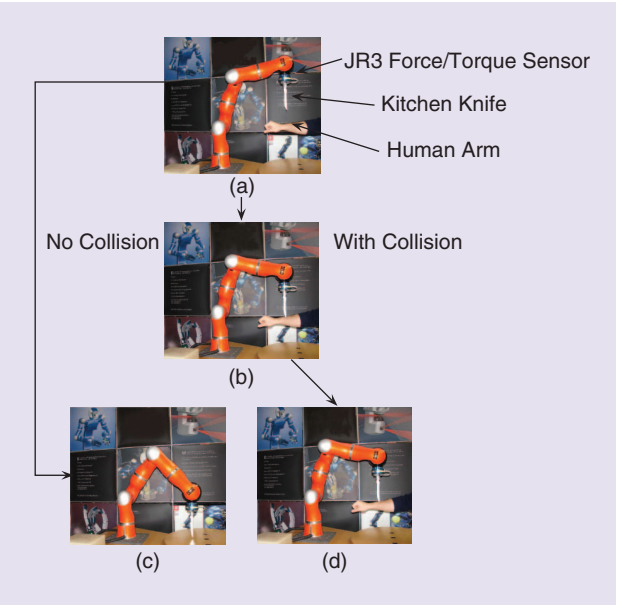

Figure 12. Effectiveness of the collision detection and reaction. The human arm is hit by the robot at $\dot{\mathbf{x}}_R \in \{0.15\ 0.25\ 0.5\ 1.0\}$ m/s. The desired trajectory of the robot is a straight line in the vertical direction. (a) Initial robot configuration. (b) The robot moves along its desired trajectory. (c) Desired goal configuration of the robot. (d) The robot detects the collision with the human arm and stops before hurting the human.

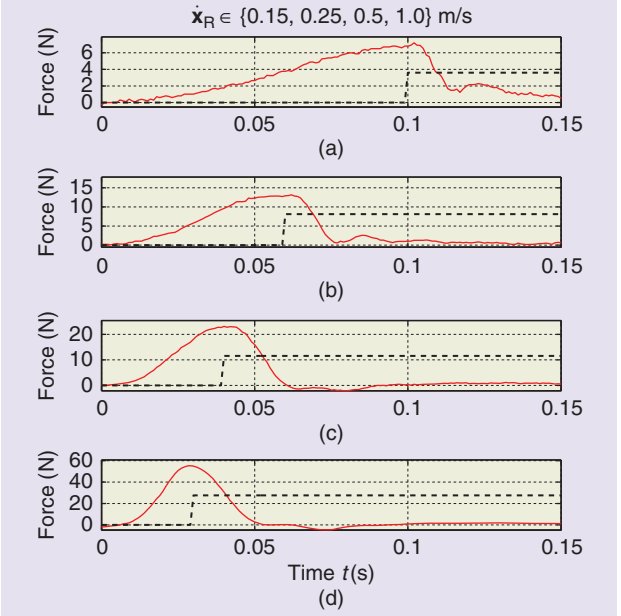

Figure 13. Stabbing tests in free space with a human volunteer. The force can be limited to subcritical values. The dashed line is the measured contact force and the dashed–dotted line is the collision detection signal.

robot is able to prevent the human from being injured at all. The contact force was limited in this experiment to 7 N for 0.15 m/s, 13 N at 0.25 m/s, 23 N at 0.5 m/s, and 55 N at 1.0 m/s. Only for 1.0 m/s, a minimal scratch in the epidermis could be observed. This experiment strongly supports the results obtained from simulation and experimental evaluations. It points out that, although intuitively it seems very unrealistic to prevent injury of humans during sharp contact by means of control, there is a clear chance to greatly reduce danger to the human up to velocities of 1.0 m/s.

Conclusions

In this article, we carried out a simulation and experimental evaluation of soft-tissue injuries in robotics. The treatment of such injuries is a fundamental and crucial precondition to our understanding to allow robots to handle sharp tools in the presence of humans. In this article, we deal with stab/puncture wounds caused by sharp tools. The fact that a knife can penetrate into deeper human inner regions and therefore threaten sensitive organs is the motivation for this evaluation. The penetration depth and the associated braking distance are identified as suitable injury and performance criteria for cutting and stabbing injury. Based on experimental investigation of various increasingly sharp tools, ranging from a screwdriver to a scalpel, a clear understanding of the relevant factors of certain types of soft-tissue injury was derived. Furthermore, our analysis clearly shows that collision detection and reaction is a powerful tool to reduce or even prevent injury. A video showing the experiments discussed in this article can be obtained from the multimedia accompanying this article in IEEE *Xplore* or from http://www.safe-robots.com/ram2011.html.

Acknowledgments

We thank Manfred Schedl for bringing up the idea of pig experiments. Our special thanks go to Prof. Dimitrios Kallieris who shares his rich biomechanical knowledge with us. Last but not least, our gratitude goes to Prof. Alessandro De Luca with whom the collision detection and reaction was developed. This work has been partially funded by the European Commission's Sixth Framework Programme as part of the project PHRIENDS under grant 045359, SAPHARI under grant 287513, and VIACTORS under grant 231554. We hereby assure that the experimental protocol was carried out in accordance to the rules of the authors' local ethical committee.

References

[1] S. Haddadin, A. Albu-Schäffer, and G. Hirzinger, "Soft-tissue injury in robotics," in *Proc. IEEE Int. Conf. Robotics and Automation (ICRA)*, Anchorage, AL, 2010, pp. 3462–3433.

[2] *Robots for Industrial Environments—Safety Requirements—Part 1: Robot*, ISO Standard 10218, 2006.

[3] V. Lumelsky and E. Cheung, "Real-time collision avoidance in teleoperated whole-sensitive robot arm manipulators," *IEEE Trans. Syst., Man Cybern.*, vol. 23, no. 1, pp. 194–203, 1993.

[4] A. De Luca, A. Albu-Schäffer, S. Haddadin, and G. Hirzinger, "Collision detection and safe reaction with the DLR-III lightweight

manipulator arm," in *Proc. IEEE/RSJ Int. Conf. Intelligent Robots and Systems (IROS)*, Beijing, China, 2006, pp. 1623–1630.
[5] J. Heinzmann and A. Zelinsky, "Quantitative safety guarantees for physical human-robot interaction," *Int. J. Robot. Res.*, vol. 22, no. 7–8, pp. 479–504, 2003.
[6] K. Ikuta, H. Ishii, and M. Nokata, "Safety evaluation method of design and control for human-care robots," *Int. J. Robot. Res.*, vol. 22, no. 5, pp. 281–298, 2003.
[7] A. De Luca and R. Mattone, "Sensorless robot collision detection and hybrid force/motion control," in *Proc. IEEE Int. Conf. Robotics and Automation (ICRA)*, Barcelona, Spain, 2005, pp. 1011–1016.
[8] D. Ebert and D. Henrich, "Safe human-robot-cooperation: Image-based collision detection for industrial robots," in *Proc. IEEE/RSJ Int. Conf. Intelligent Robots and Systems (IROS)*, Lausanne, Switzerland, 2002, pp. 239–244.
[9] S. Morinaga and K. Kosuge, "Collision detection system for manipulator based on adaptive impedance control law," in *Proc. IEEE Int. Conf. Robotics and Automation (ICRA)*, Washington, DC, 2002, pp. 1080–1085.
[10] Y. Yamada, Y. Hirasawa, S. Huand, and Y. Umetani, "Fail-safe human/robot contact in the safety space," in *Proc. IEEE Int. Workshop Robot and Human Communication*, 1996, pp. 59–64.
[11] M. Zinn, O. Khatib, B. Roth, and J. Kalisbury, "Playing it safe—Human-friendly robots," *IEEE Robot. Automat. Mag.*, vol. 11, no. 2, pp. 12–21, 2002.
[12] A. Bicchi and G. Tonietti, "Fast and soft arm tactics: Dealing with the safety-performance trade-off in robot arms design and control," *IEEE Robot. Automat. Mag.*, vol. 11, no. 2, pp. 22–33, 2004.
[13] S. Haddadin, A. Albu-Schäffer, and G. Hirzinger, "Safety evaluation of physical human-robot interaction via crash-testing," in *Proc. Robotics: Science and Systems Conf. (RSS)*, Atlanta, GA, 2007, pp. 217–224.
[14] S. Haddadin, A. Albu-Schäffer, and G. Hirzinger, "The role of the robot mass and velocity in physical human-robot interaction—Part I: Unconstrained blunt impacts," in *Proc. IEEE Int. Conf. Robotics and Automation (ICRA)*, Pasadena, CA, 2008, pp. 1331–1338.
[15] S. Haddadin, A. Albu-Schäffer, and G. Hirzinger, "The role of the robot mass and velocity in physical human-robot interaction—Part II: Constrained blunt impacts," in *Proc. IEEE Int. Conf. Robotics and Automation (ICRA)*, Pasadena, CA, 2008, pp. 1339–1345.
[16] K. T. Ulrich, T. T. Tuttle, J. P. Donoghue, and W. T. Townsend, (1995, May). Intrinsically safer robots. Barrett Technology, Cambridge, MA, Tech. Rep. NAS10-12178 [Online]. Available: http://www.barrett.com/robot/
[17] P. I. Corke, "Safety of advanced robots in human environments. A discussion paper," in *Proc. Int. Advanced Robotics Programme*, 1999.
[18] M. Wassink and S. Stramigioli, "Towards a novel safety norm for domestic robots," in *Proc. IEEE/RSJ Int. Conf. Intelligent Robots and Systems (IROS)*, San Diego, CA, 2007, pp. 3354–3359.
[19] S. Haddadin, A. Albu-Schäffer, and G. Hirzinger, "Safe physical human-robot interaction: Measurements, analysis and new insights," in *Proc. Robotics Research: The 13th Int. Symp. (ISRR)*, M. Kaneko and Y. Nakamura, Eds. Berlin: Springer-Verlag, 2010, pp. 395–408.
[20] D. Kallieris, *Handbuch gerichtliche Medizin—Biomechanik*. Berlin: Springer Verlag, 2004.
[21] I. Fazekas, F. Kosa, I. Bajnoczky, G. Jobba, and J. Szendrenyi, "Mechanische Untersuchung der Kraft durchbohrender Einstiche an der menschlichen Haut und verschiedenen Kleidungsschichten," *Zeitschrift für Rechtsmedizin*, vol. 70, no. 4, pp. 235–240, 1972.
[22] W. Weber and H. Schweitzer, "Stichversuche an Leichen mit unterschiedlicher kinetischer Energie," *Beiträge Gerichtliche Medizin*, vol. 31, pp. 180–184, 1973.
[23] A. von Prittwitz und Gaffron, "Bestimmung der Kraft durchbohrender Einstiche am menschlichen Thorax mit einem 'in situ'—Messverfahren," Ph.D. dissertation, Univ. of Heidelberg, 1974.
[24] W. Eisenmenger, *Handbuch gerichtliche Medizin—Spitze, scharfe und halbscharfe Gewalt*, B. Brinkmann and B. Madea, Eds. Berlin, Germany: Springer-Verlag, 2004.
[25] S. Haddadin, A. Albu-Schäffer, A. De Luca, and G. Hirzinger, "Collision detection and reaction: A contribution to safe physical human-robot interaction," in *Proc. IEEE/RSJ Int. Conf. Intelligent Robots and Systems (IROS)*, Nice, France, 2008, pp. 3356–3363.
[26] G. Hirzinger, N. Sporer, A. Albu-Schäffer, R. Krenn, A. Pascucci, and M. Schedl, "DLR's torque-controlled light weight robot III—Are we reaching the technological limits now?" in *Proc. ICRA*, 2002, pp. 1710–1716.
[27] A. Albu-Schäffer, S. Haddadin, C. Ott, A. Stemmer, T. Wimböck, and G. Hirzinger, "The DLR lightweight robot lightweight design and soft robotics control concepts for robots in human environments," *Indust. Robot J.*, vol. 34, no. 5, pp. 376–385, 2007.
[28] S. Haddadin, "Evaluation criteria and control structures for safe human-robot interaction," M.S. thesis, Tech. Univ. of Munich & German Aerospace Center (DLR), Munich, Germany, Dec. 2005.
[29] A. De Luca and R. Mattone, "An adapt-and-detect actuator FDI scheme for robot manipulators," in *Proc. IEEE Int. Conf. Robotics and Automation (ICRA)*, New Orleans, LA, 2004, pp. 4975–4980.
[30] A. Albu-Schäffer, C. Ott, and G. Hirzinger, "A unified passivity-based control framework for position, torque and impedance control of flexible joint robots," *Int. J. Robot. Res.*, vol. 26, no. 1, pp. 23–39, 2007.
[31] A. Albu-Schäffer and G. Hirzinger, "Cartesian impedance control techniques for torque controlled light-weight robots," in *Proc. IEEE Int. Conf. Robotics and Automation (ICRA)*, Washington, DC, 2002, pp. 657–663, 2002.
[32] M. Spong, "Modeling and control of elastic joint robots," *IEEE J. Robot. Automat.*, vol. 3, no. 4, pp. 291–300, 1987.

Sami Haddadin, Institute of Robotics and Mechatronics, DLR - German Aerospace Center, Wessling, Germany. E-mail: sami.haddadin@dlr.de.

Alin Albu-Schäffer, Institute of Robotics and Mechatronics, DLR - German Aerospace Center, Wessling, Germany. E-mail: alin.albu-schaeffer@dlr.de.

Fahed Haddadin, Group Practice Onkology and Inner Medicine, Garbsen, Germany. E-mail: haddadin@onkologie-garbsen.de.

Jürgen Roßmann, Institute of Man–Machine Interaction, Rheinisch-Westfälische Technische Hochschule Aachen (RWTH), Aachen, Germany. E-mail: rossmann@mmi.rwth-aachen.de.

Gerd Hirzinger, Institute of Robotics and Mechatronics, DLR - German Aerospace Center, Wessling, Germany. E-mail: gerd.hirzinger@dlr.de.